THE JOURNAL OF PHYSICAL CHEMISTRY A

Article

pubs.acs.org/JPCA

Electronic Flux Density beyond the Born−Oppenheimer Approximation

Axel Schild,* Federica Agostini, and E. K. U. Gross

Max-Planck Institut für Mikrostrukturphysik, Weinberg 2, D-06120 Halle, Germany

ABSTRACT: In the Born−Oppenheimer approximation, the electronic wave function is typically real-valued and hence the electronic flux density (current density) seems to vanish. This is unfortunate for chemistry, because it precludes the possibility to monitor the electronic motion associated with the nuclear motion during chemical rearrangements from a Born−Oppenheimer simulation of the process. We study an electronic flux density obtained from a correction to the electronic wave function. This correction is derived via nuclear velocity perturbation theory applied in the framework of the exact factorization of electrons and nuclei. To compute the correction, only the ground state potential energy surface and the electronic wave function are needed. For a model system, we demonstrate that this electronic flux density approximates the true one very well, for coherent tunneling dynamics as well as for over-the-barrier scattering, and already for mass ratios between electrons and nuclei that are much larger than the true mass ratios.

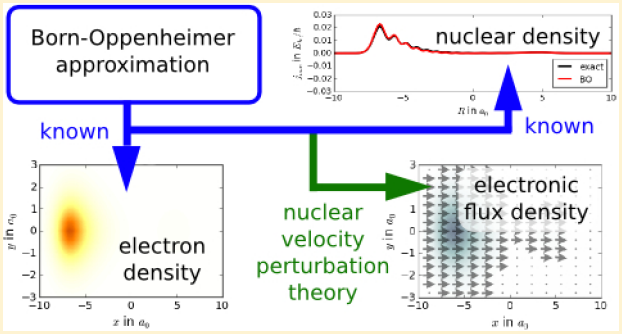

INTRODUCTION

In the Born−Oppenheimer (BO) approximation,[1] the electrons are assumed to be fast enough (or the nuclei slow enough) so that from their perspective, the nuclei can be considered as frozen. Hence, the total wave function $\Psi(\mathbf{R},\mathbf{r},t)$ of a molecule is written as

$$\Psi(\mathbf{R},\mathbf{r},t) \approx \chi^{\mathrm{BO}}(\mathbf{R},t)\, \Phi^{\mathrm{BO}}(\mathbf{r}|\mathbf{R}) \tag{1}$$

i.e., as a product of a time-dependent nuclear wave function $\chi^{\mathrm{BO}}(\mathbf{R},t)$ and a stationary electronic wave function $\Phi(\mathbf{r}|\mathbf{R})$, which depends on the electronic coordinates $\mathbf{r}$ and parametrically on the nuclear positions $\mathbf{R}$, but not on the time t. In a time-dependent situation, this view has interesting consequences for the internal motion of the molecule: Because the electronic wave function depends only on the position but not on the velocity of the nuclei, information about the electronic motion is missing. Although the time-dependent electron density

$$\rho^{\mathrm{BO}}(\mathbf{r},t) = \int |\chi^{\mathrm{BO}}(\mathbf{R},t)|^2 |\Phi^{\mathrm{BO}}(\mathbf{r}|\mathbf{R})|^2 \, \mathrm{d}\mathbf{R} \tag{2}$$

that in the BO picture is induced by the motion of the nuclei is a very good approximation to the exact one, the electronic flux density (also called electronic current density) computed from the standard expression in general gives[2,3]

$$\mathbf{j}^{\mathrm{BO}}(\mathbf{r},t) = 0 \tag{3}$$

We refer here to the time-dependent density and flux density after separation of translational and approximate separation of rotational degrees of freedom of the system, and we do not consider currents induced by external fields or related to nonzero electronic angular momenta.

That the electronic flux density is zero for the BO wave function is unfortunate, especially for chemistry. Typically, chemists like to think in terms of reaction mechanisms; i.e., they want to know how the electrons move during the course of a reaction. For this purpose, the electronic flux density is necessary because it shows the direction of the electronic motion. In a semiclassical study of proton transfer in formamide, for example, the electronic flux density revealed the mechanism and showed that the electrons move in the opposite direction to the motion of the proton.[4] Additionally, time-dependent extensions for the concept of a chemical bond may also need the electronic flux density: For example, the electron localization function is based on the static BO electronic wave function,[5] but the definition of the time-dependent electron localization function contains the electronic flux density.

Another problem where the electronic flux density is (implicitly) needed is for vibrational circular dichroism, a spectroscopic technique that relies on the interaction of chiral media with circularly polarized light.[6] To predict the spectrum, it is necessary to compute the magnetic transition dipole moments, which are zero in the BO treatment for the same reason as the electronic flux density. Thus, a correction to the electronic BO wave function that yields the correct vibrational

Special Issue: Ronnie Kosloff Festschrift

Received: December 28, 2015
Revised: February 13, 2016
Published: February 15, 2016

DOI: 10.1021/acs.jpca.5b12657
J. Phys. Chem. A 2016, 120, 3316−3325

circular dichroism spectrum also yields the correct electronic flux density.

Several approaches to remedy this problem were put forward. A first approach was the time-shift flux.[7] In essence, it proposes to compute a flux density from the wave function at time t and time $t + \Delta t$, to obtain information about the electronic motion. In the same spirit, the Born−Oppenheimer broken symmetry ansatz[8] suggests using the wave function at nuclear configurations $\mathbf{R}$ and $\mathbf{R} + \Delta\mathbf{R}$. This ansatz seems promising to represent the qualitative features of the electronic flux density in a computationally inexpensive way. Another approach is the coupled-channels theory[9−12] that uses the atomic basis sets employed in computing the electronic wave function to suggest an electronic flux density. However, the applicability of the coupled-channels theory is restricted, which resulted in the development of a quasi-classical approach[13] and a "non-BO approximation",[14] where the latter has some similarities to our approach. We comment on the these below. As an alternative to the flux density, one may use the electronic flux defined relative to a certain volume in the electronic configuration space to investigate chemical reactions,[15−17] albeit this approach has limitations in the absence of a useful spatial symmetry.[18]

In this article, we investigate an electronic flux density that is obtained from a correction to the electronic wave function. This correction is the result of nuclear velocity perturbation theory (NVPT)[19] and was recently derived[20] from the exact factorization of electrons and nuclei.[21,22] A related approach for classical nuclei was proposed by Nafie[23] as the "complete adiabatic wavefunction" and recently implemented for the problem of the electronic flux density[24] and for the problem of vibrational circular dichroism.[25] The derivation from the exact factorization is the quantum-mechanical generalization of this approach. It also shows why the NVPT electronic flux density is useful in the BO approximation: From the exact factorization follows that it originates from a first-order correction in the same parameter that also determines the validity of the BO approximation. The parameter can be interpreted classically as the nuclear velocity but has a more general meaning when analyzed in the framework of the exact factorization.[20] Hence, the NVPT electronic flux density is expected to be a good approximation to the true electronic flux density whenever the BO dynamics is a good approximation to the true molecular dynamics. Additionally, the correction of the electronic wave function does (to first order) neither alter the potential energy surface that determines the dynamics of the nuclei nor are excited BO electronic states necessary for its computation (albeit they can be used, as shown below).

So far no systematic study on the quality of the NVPT correction to the electronic flux density has been performed. In this article, we provide such a study based on the analysis of a model system. Exact solutions for molecular systems are difficult to compute because of the large number of particles involved and because of the different masses of electrons and nuclei that require different time scales for the simulation. We simulate the coupled dynamics of a heavy particle and an electron tunneling through or scattering from a barrier, and we investigate the quality of the electronic flux density for different values of the ratio between the mass of the electron and of the heavy particle. Additionally, we compare two ways to compute the NVPT correction: One possibility is to use the electronic ground-state wave function and potential energy surface. It is then necessary to solve a system of equations that involves the derivative of the electronic wave function with respect to the nuclear coordinates. Another possibility is to use an expansion in excited states. We examine the convergence with the number of included excited states in this expansion to determine whether only a small number of states can already yield a qualitatively correct electronic flux density. For the study of reaction mechanisms in complicated systems, a qualitative picture can already be enough to understand the process and develop or test general concepts.

THE ELECTRONIC FLUX DENSITY IN THE BORN−OPPENHEIMER APPROXIMATION

In what follows, we assume that after separation of the center of mass and approximate separation of the rotational degrees of freedom of the total molecule, the wave function can be written as an approximate product of three terms, corresponding to the linear, rotational, and internal motion of the molecule. Next, we assume that the linear and rotational part correspond to narrow distributions. Thus, we say that our molecule has a well-defined location and orientation in space, to avoid a constant or rotationally symmetric electron density. We neglect the ensuing problem of the coupling of internal motions to the rotation of the system[26] based on the assumption that the dynamics of interest is faster than the effect of the coupling. The exact approach to define internal coordinates of the nuclei and the electronic coordinates relative to the molecular center of mass, and to transform the total Hamiltonian accordingly, will not be pursued here because of its many complications.[27] Clearly, the proper inclusion of the coupling between rotations and vibrations deserves further attention.

For a molecular system, coupled motion of electrons and nuclei is described by the time-dependent Schrödinger equation

$$i\hbar\partial_t\Psi(\mathbf{R},\mathbf{r},t) = (T_n + H_{BO})\Psi(\mathbf{R},\mathbf{r},t) \tag{4}$$

where T_n is the nuclear kinetic energy and H_{BO} is the BO Hamiltonian containing the electronic kinetic energy and all Coulomb interactions. The system is composed of N_n nuclei with masses M_ν and coordinates $\mathbf{R}_\nu$, and N_e electrons with coordinates $\mathbf{r}_j$. We will work with the electronic N_e-particle density (normalized to one) and the electronic N_e-particle flux density, which will in the following be simply called electron density and electron flux density. The more practical one-electron density and one-electron flux density can be obtained by integrating over all but one electronic coordinate in the relevant equations. We need the spatial derivatives for each nucleus ν, denoted with ∇_ν, and with respect to all electronic coordinates, denoted with $\partial_\mathbf{r}$. The electron density is

$$\rho(\mathbf{r},t) = \int |\Psi(\mathbf{R},\mathbf{r},t)|^2 \, d\mathbf{R} \tag{5}$$

From the Schrödinger equation and the continuity equation for the density $|\Psi|^2$ it follows that the electronic flux density is given by

$$\mathbf{j}(\mathbf{r},t) = \frac{\hbar}{m_e}\int \Im(\Psi^*\partial_\mathbf{r}\Psi) \, d\mathbf{R} \tag{6}$$

In the BO approximation, the molecular wave function is written as

$$\Psi(\mathbf{R},\mathbf{r},t) = \chi^{BO}(\mathbf{R},t)\,\Phi_0^{BO}(\mathbf{r}|\mathbf{R}) \tag{7}$$

where Φ_0 is the lowest energy solution[a] of

DOI: 10.1021/acs.jpca.5b12657
J. Phys. Chem. A 2016, 120, 3316−3325

$$H_{\mathrm{BO}}(\mathbf{R})\,\Phi_j^{\mathrm{BO}}(\mathbf{r}|\mathbf{R}) = \epsilon_j^{\mathrm{BO}}(\mathbf{R})\,\Phi_j^{\mathrm{BO}}(\mathbf{r}|\mathbf{R}) \tag{8}$$

and, instead of (4), the time evolution of the nuclear wave function is described by

$$\mathrm{i}\hbar\partial_t\chi^{\mathrm{BO}}(\mathbf{R},t) = (T_{\mathrm{n}} + \epsilon_j^{\mathrm{BO}}(\mathbf{R}))\chi^{\mathrm{BO}}(\mathbf{R},t) \tag{9}$$

Using the Born−Oppenheimer ansatz (7) in the definition of the electron density (5) yields

$$\rho^{\mathrm{BO}}(\mathbf{r},t) = \int |\chi^{\mathrm{BO}}(\mathbf{R},t)\,\Phi_0^{\mathrm{BO}}(\mathbf{r}|\mathbf{R})|^2\,\mathrm{d}\mathbf{R} \tag{10}$$

which was found to be a very good approximation to the true electron density.[2] In contrast, inserting (7) into the definition of the electronic flux density (6) yields

$$\mathbf{j}^{\mathrm{BO}}(\mathbf{r},t) = 0 \tag{11}$$

if the electronic ground state Φ_0 is nondegenerate.[2] Obviously, because the density ρ^{BO} changes in time, the flux density $\mathbf{j}^{\mathrm{BO}}$ cannot be the corresponding flux density, as it yields zero flux everywhere. In the following, we correct the electronic wave function by perturbation theory to obtain a nonzero electronic flux density that is a good approximation to the true one whenever the BO approximation is valid for the dynamics of the system. The exact factorization is used to identify the proper perturbation parameter.

EXACT FACTORIZATION OF THE ELECTRON−NUCLEAR WAVE FUNCTION

In the exact factorization, the molecular wave function is written as

$$\Psi(\mathbf{R},\mathbf{r},t) = \chi(\mathbf{R},t)\,\Phi(\mathbf{r},t|\mathbf{R}) \tag{12}$$

with partial normalization condition $\langle\Phi|\Phi\rangle_{\mathbf{r}} = 1\ \forall\mathbf{R}, t$, with $\langle\ldots\rangle_{\mathbf{r}}$ indicating integration over the electronic coordinates. In contrast to (7), the decomposition into a marginal nuclear wave function χ and a conditional electronic wave function Φ does not involve an approximation. The theory and interpretation of the exact factorization have been extensively presented elsewhere.[21,22,28−45] Therefore, we recall here only the basic ideas and we focus on a discussion of the approximations employed in the following analysis.

Using the exact factorization ansatz (12) together with the time-dependent Schrödinger equation (4) yields two coupled evolution equations for the two components of the full wave function,

$$(H_{\mathrm{BO}} + U[\Phi,\chi] - \epsilon(\mathbf{R},t))\Phi(\mathbf{r},t|\mathbf{R}) = \mathrm{i}\hbar\partial_t\Phi(\mathbf{r},t|\mathbf{R}) \tag{13}$$

$$\left(\sum_{\nu=1}^{N_n}\frac{[-\mathrm{i}\hbar\nabla_\nu + \mathbf{A}_\nu(\mathbf{R},t)]^2}{2M_\nu} + \epsilon(\mathbf{R},t)\right)\chi(\mathbf{R},t) = \mathrm{i}\hbar\partial_t\chi(\mathbf{R},t) \tag{14}$$

Note that $|\chi|^2$ is the exact nuclear many-body density and χ together with $\mathbf{A}_\nu$ also yield the exact nuclear flux density. The electron−nuclear coupling operator

$$U[\Phi,\chi] = \sum_{\nu=1}^{N_n}\frac{1}{M_\nu}\left[\frac{[-\mathrm{i}\hbar\nabla_\nu - \mathbf{A}_\nu]^2}{2} + \left(\frac{-\mathrm{i}\hbar\nabla_\nu\chi}{\chi} + \mathbf{A}_\nu\right)\cdot(-\mathrm{i}\hbar\nabla_\nu - \mathbf{A}_\nu)\right] \tag{15}$$

is the source of the nonadiabatic coupling to the nuclei. Similarly, the time-dependent vector potential (TDVP) and time-dependent potential energy surface (TDPES), defined as

$$\mathbf{A}_\nu(\mathbf{R},t) = \langle\Phi|\,-\mathrm{i}\hbar\nabla_\nu\,\Phi\rangle_{\mathbf{r}} \tag{16}$$

$$\epsilon(\mathbf{R},t) = \langle\Phi|H_{\mathrm{BO}} + U - \mathrm{i}\hbar\partial_t|\Phi\rangle_{\mathbf{r}} \tag{17}$$

respectively, induce the coupling to the electrons in the nuclear evolution eq 14. There is a gauge freedom in the exact factorization, because for some function $S(\mathbf{R},t)$ the wave functions $\tilde{\chi} = \mathrm{e}^{-\mathrm{i}S}\chi$ and $\tilde{\Phi} = \mathrm{e}^{\mathrm{i}S}\Phi$ leave the full wave function (12) and the equations of motion invariant, if the scalar and vector potentials satisfy the gauge transformation

$$\tilde{A}_\nu = \mathbf{A}_\nu + \nabla_\nu S \tag{18}$$

$$\tilde{\epsilon} = \epsilon + \partial_t S \tag{19}$$

It is evident that if the coupling U is zero and the initial electronic state is chosen to be an eigenstate Φ_j^{BO} of H_{BO} (8), the electronic equation (13) reproduces the evolution of a stationary state. Therefore, if the ground state Φ_0^{BO} is considered, the BO approximation is recovered, i.e., the potential obtained from the (13) and used in the nuclear equation (14) is the ground state potential ϵ_0^{BO}.

CORRECTIONS TO THE BORN−OPPENHEIMER ELECTRONIC WAVE FUNCTION FROM NUCLEAR VELOCITY PERTURBATION THEORY

To make progress regarding the electronic flux density, we neglect those parts of U that do not directly couple to the nuclear wave function, i.e., the first term in (15).[46] We do this because U has a factor $1/M_\nu$ that is typically a very small number, and for the first term in (15) this factor cannot be compensated by features of the nuclear wave function. Then, the electron−nuclear coupling operator (15) becomes

$$U[\Phi_{\mathbf{R}},\chi] \simeq \sum_{\nu=1}^{N_n}\boldsymbol{\lambda}_\nu\cdot(-\mathrm{i}\hbar\nabla_\nu - \mathbf{A}_\nu) \tag{20}$$

with the velocity field

$$\boldsymbol{\lambda}_\nu(\mathbf{R},t) = \frac{1}{M_\nu}\left(\frac{-\mathrm{i}\hbar\nabla_\nu\chi}{\chi} + \mathbf{A}_\nu\right) \tag{21}$$

In this approximation, the coupling operator U does not contribute to the exact potential ϵ, as the expectation value of (20) with respect to the electronic wave function Φ is zero.

The field $\boldsymbol{\lambda}_\nu$ will be used below as expansion parameter, because it represents the coupling of the nuclear wave function to the electronic wave function. It should be noted that only the real part of $\boldsymbol{\lambda}_\nu$ is the velocity field of the nuclei, which is given by the nuclear flux density

$$\mathbf{J}_\nu(\mathbf{R},t) = \frac{1}{M_\nu}(\hbar\,\mathrm{Im}(\chi^*\nabla_\nu\chi) + |\chi|^2\mathbf{A}_\nu) \tag{22}$$

divided by the nuclear density $\rho(\mathbf{R},t) = |\chi|^2$. Additionally, there is an imaginary part that depends on the gradient of the density. Specifically,

$$\boldsymbol{\lambda}_\nu(\mathbf{R},t) = \frac{\mathbf{J}_\nu}{\rho} + \frac{\hbar}{2\mathrm{i}M_\nu}\frac{\nabla_\nu\rho}{\rho} \tag{23}$$

DOI: 10.1021/acs.jpca.5b12657
J. Phys. Chem. A 2016, 120, 3316−3325

Hence, for λ_ν to be small, both the velocity field of the nuclei and the variation of the nuclear density in space have to be small.

We have previously[33,34] argued that in the classical limit[47] of the nuclear wave function, λ_ν can be approximated as the classical nuclear velocity, $\lambda_\nu(\mathbf{R},t) \simeq \dot{\mathbf{R}}_\nu(t)$, and this observation was the starting point[20] for the introduction of the NVPT[19] in the framework of the exact factorization. The basic idea can be summarized in the following way: (i) if $\lambda_\nu = 0$, the BO limit is recovered, as described above; (ii) if $\lambda_\nu \gg 0$, the dynamics is nonadiabatic, and the effect of the nuclei is fully accounted for by the coupling operator U of (20); (iii) if λ_ν is small, nonadiabatic effects can be taken into account as a perturbation to the BO limit. When the adiabatic approximation is invoked, the electronic problem is solved at fixed nuclear position, meaning that the velocity of the nuclei (the classical limit of λ_ν) is zero. If the velocity is small, or similarly if λ_ν is small, we can expect a small deviation from the adiabatic behavior, which can be treated perturbatively.

We want to point out that the correction for classical nuclei was previously also found by Nafie[23] and, later, by Patchkovskii.[24] Compared to their approaches, our derivation from the exact factorization has two advantages: As our result is derived for quantum-mechanical nuclei, it is possible to obtain corrections to the classical limit that include quantum effects. Additionally, the expansion parameter appears naturally when the BO equations are compared with the equations of the exact factorization. From this comparison, it is evident that the expansion parameter has to be small both for the BO approximation to hold and for the NVPT correction to be applicable. Thus, the derivation shows that the NVPT correction is appropriate whenever the BO approximation is appropriate, for quantum and for classical nuclei.

Henceforth, we will work in a gauge where the exact TDVP $\mathbf{A}_\nu(\mathbf{R},t) = 0$. This choice of gauge is not possible if $\nabla_\nu \times \mathbf{A}_\nu \neq 0$, and Berry phase effects may be important.[37,48] Then, the analysis presented below might have to be extended.

We consider the electronic equation (13) with approximate electron−nuclear coupling (20),

$$[H_{\mathrm{BO}} + \sum_{\nu=1}^{N_n} \lambda_\nu(\mathbf{R},t)\cdot(-\mathrm{i}\hbar\nabla_\nu)]\Phi(\mathbf{r},t|\mathbf{R}) = \epsilon(\mathbf{R},t)\,\Phi(\mathbf{r},t|\mathbf{R}) \tag{24}$$

and solve it within perturbation theory. We did not use new symbols in (24), but it should be kept in mind that we are not using the full coupling operator; hence, the electronic wave function Φ and in consequence also the TDPES ϵ are only (typically very good) approximations to the exact quantities. Note that in writing (24), we discard the time-derivative of the electronic wave function that occurs in (13). In doing this, we adopt the hypothesis that the electronic wave function is almost a static state of the BO electronic wave function.[19,20] We set

$$\Phi(\mathbf{r},t|\mathbf{R}) = \Phi^{(0)} + \mathrm{i}\sum_{\nu=1}^{N_n} \lambda_\nu\cdot\mathbf{\Phi}_\nu^{(1)} + O(\lambda_\nu^{\,2}) \tag{25}$$

To zeroth order in λ_ν,

$$H_{\mathrm{BO}}\Phi^{(0)} = \epsilon^{(0)}\Phi^{(0)} \tag{26}$$

hence, $\epsilon^{(0)} = \epsilon_0^{\mathrm{BO}}(\mathbf{R})$ and $\Phi^{(0)} = \Phi_0^{\mathrm{BO}}(\mathbf{r}|\mathbf{R})$ are the time-independent BO ground-state potential and eigenfunction. To first order in λ_ν, we find

$$(H_{\mathrm{BO}} - \epsilon_0^{\mathrm{BO}})\mathbf{\Phi}_\nu^{(1)}(\mathbf{r}|\mathbf{R}) = \hbar\nabla_\nu\Phi_0^{\mathrm{BO}} \tag{27}$$

The first-order correction to the BO ground-state wave function is straightforward to calculate from this expression, because only the ground-state wave function and the ground-state potential are needed.

Some observations need to be made: The TDPES is not affected by the perturbation at first order, i.e., $\epsilon(\mathbf{R},t) = \epsilon_0^{\mathrm{BO}}(\mathbf{R}) + O(\lambda_\nu^{\,2})$. Also, although within the BO picture we work in a gauge where the exact TDVP $\mathbf{A}_\nu = 0$, there is a nonzero contribution of the TDVP to first order in λ_ν. To be fully consistent, we would have to include this correction in the determination of the nuclear dynamics in (9). Instead, we neglect this contribution and use the BO nuclear wave function determined with zero vector potential, as is typically done in practice.

Next, we expand $\mathbf{\Phi}_\nu^{(1)}$ in terms of excited BO electronic states, so that (25) becomes

$$\Phi(\mathbf{r},t|\mathbf{R}) = \Phi^{(0)} + \mathrm{i}\hbar\sum_{\nu=1}^{N_n}\lambda_\nu\cdot\sum_{j>0}\frac{\mathbf{d}_{j0,\nu}}{\epsilon_j^{\mathrm{BO}} - \epsilon_0^{\mathrm{BO}}}\Phi_j^{\mathrm{BO}} + O(\lambda_\nu^{\,2}) \tag{28}$$

where

$$\mathbf{d}_{j0,\nu}(\mathbf{R}) = \langle\Phi_j^{\mathrm{BO}}(\mathbf{R})|\nabla_\nu\Phi_0^{\mathrm{BO}}(\mathbf{R})\rangle_{\mathbf{r}} \tag{29}$$

is the nonadiabatic coupling vector corresponding to νth nucleus between the BO states j and 0. We emphasize that our approach aims at obtaining the electronic flux density in situations where the BO approximation is a good description of the dynamics. In the vicinity of a conical intersection (28) diverges. Clearly, this case is excluded by the assumptions.

Thus, we have determined two ways to compute the correction $\mathbf{\Phi}_\nu^{(1)}$ to the BO electronic wave function: We solve (27), e.g., by determining the gradient of Φ_0^{BO} at each configuration $\mathbf{R}$, and then solve the matrix equation with the ground state potential at those positions. Alternatively, if excited states are available, we directly calculate the correction from (28). This approach may be computationally preferred if the convergence with respect to the number of included excited states is sufficiently good and only a qualitative picture of the electronic flux density is of interest.

Finally, from the correction to the electronic wave function follows that the NVPT electronic flux density to first order in λ_ν is given by

$$\mathbf{j}^{\mathrm{NVPT}}(\mathbf{r},t) = \frac{\hbar}{m_{\mathrm{e}}}\int(\Phi_0^{\mathrm{BO}}\partial_{\mathbf{r}}\tilde{\Phi}^{(1)} - \tilde{\Phi}^{(1)}\partial_{\mathbf{r}}\Phi_0^{\mathrm{BO}})\,\mathrm{d}\mathbf{R} \tag{30}$$

with

$$\tilde{\Phi}^{(1)}(\mathbf{R},\mathbf{r},t) = \sum_{\nu=1}^{N_n}\mathbf{J}_\nu(\mathbf{R},t)\cdot\mathbf{\Phi}_\nu^{(1)}(\mathbf{r}|\mathbf{R}) \tag{31}$$

Below, we will test the convergence of the electronic flux density with respect to the number of included excited states to see which way to compute the correction may be more efficient.

In summary, we represent the molecular wave function by the exact factorization ansatz and apply perturbation theory to the electronic part only, with the approximate electron−nuclear coupling operator (20) as perturbation. An alternative approach is presented by Diestler[14] who expands the molecular wave

DOI: 10.1021/acs.jpca.5b12657
J. Phys. Chem. A 2016, 120, 3316−3325

function in terms of BO states and uses the nuclear kinetic energy operator as perturbation. Then, an "average excitation energy" approximation is used to find an equation for the molecular wave function (eq 5.18 in ref 14) and an equation for the electronic flux density (eq 7.5 in ref 14) that are similar to our results (28) and (30), respectively. The main difference for the flux density is that we obtain our correction to the electronic wave function from (27) whereas the effect of the "average excitation energy" approximation is to replace the operator $H_{BO} - \epsilon_0^{BO}$ by an energy ΔE.

A MODEL STUDY

We work with atomic units; i.e., energy is given in Hartree (E_h), length is given in Bohr (a_0), mass is given in electron mass (m_e), and action is given in Planck's constant $\hbar$.

In this section, we want to systematically study the NVPT electronic flux density (30) with NVPT electronic wave function obtained either from (27), where only the electronic ground state potential and wave function are needed, or from the expansion in terms of excited electronic states (28). In actual calculations, the sum over excited states has to be truncated. Therefore, we investigate (i) how many excited states are needed in the expansion (28) until a reasonable flux density is obtained, (ii) how well (27) approximates the exact electronic flux density, because it contains the contributions from all excited states up to first order in the expansion parameter λ_ν but requires only knowledge of the ground state electronic wave function and potential energy surface, and (iii) how sensitive the electronic flux density is to the mass ratio between electron and heavy particle. We will also compare to the classical situation, i.e., reducing the nuclear wave function to a position and a velocity.

For this purpose, we construct a model that includes both nuclear and electron dynamics and can be solved numerically exactly. Our system is composed of two particles in two dimensions (X, Y): One positively charged heavy particle of mass M, hereafter called nucleus, with coordinates (R, 0) that is only allowed to move in X-direction, and one negatively charged particle of mass $m = 1\ m_e$ with coordinates (x, y) that is allowed to move in the whole plane. The interaction is modeled with Coulomb potentials including softening parameters. In addition, there is a very heavy nucleus clamped at the origin, whose Coulomb potential acts as a barrier at (0, 0) for the movable nucleus. The motion of the latter is in addition confined by a quartic well. Thus, the potential is given by

$$V = -\frac{1}{\sqrt{x^2 + y^2 + \alpha_2}} + \left(\frac{R}{R_0}\right)^4 + \frac{1}{\sqrt{R^2 + \beta}} - \frac{1}{\sqrt{(R - x)^2 + y^2 + \alpha_1}} \tag{32}$$

We chose the parameters $\alpha_1 = 0.5\ a_0^2$, $\alpha_2 = \beta = 4\ a_0^2$, and $R_0 = 12\ a_0$. With these parameters, the potential $V(R,x,y)$ has two equivalent minima and can be used to describe both coherent tunneling dynamics as well as scattering at a barrier.

It is quite clear that our model potential describes the essentials of coupled electron−proton transfer,[49] especially if we allow for more flexibility in the function describing the barrier. Also, it can be used as a model for hydrogen entering a metal.[50] For the purpose of the present article, however, it suffices as a model of a generic situation that is described typically in the BO approximation. To challenge the BO approximation, we use small masses for the nucleus, between 10 m_e and 50 m_e. A side effect of this choice is that any mass-dependent effect is much more sensitive to a variation of the mass than if we would use masses of real nuclei.

We use a grid with $R \in [-15, +15]\ a_0$, $x \in [-20, +20]\ a_0$, and $y \in [-10, +10]\ a_0$, with $n_R = 301$, $n_x = 101$, and $n_y = 51$ points, respectively. For eigenvalue problems, a finite difference approximation for the derivatives is used. The time-dependent propagation was obtained numerically by using the action of the time propagator on the wave function. In both cases, the SciPy sparse linear algebra package[51] was used, which employs the ARPACK software[52] for the solution of the eigenvalue problem and the method of refs 53 and 54 for computing the action of a matrix exponential on a matrix.

Tunneling Regime. The potential V has two equivalent minima along R, relative to the barrier at $R = 0$. We call the minimum at $R > 0$ the right minimum and the minimum at $R < 0$ the left minimum, respectively. The two minima give rise to tunneling doublets, i.e., pairs of almost degenerate states. For example, for $M = 50\ m_e$ we find that the lowest two states differ in energy only by $\Delta E_{01} = E_1 - E_0 = 2.6 \times 10^{-6} E_h$, whereas the difference between these states and the next set of almost degenerate states is $\Delta E_{12} = 0.02 E_h$. The tunneling time is defined as

$$\tau = \frac{h}{\Delta E_{01}} \tag{33}$$

As a first test, we investigate the coherent tunneling dynamics, i.e., the dynamics of a tunneling doublet without dissipation.

Our initial state is a superposition of the lowest two eigenstates of the full Hamiltonian, ψ_0 and ψ_1, with phases defined such that the wave function is localized at the right minimum. The time-dependent wave function is thus given by

$$\psi(R,x,y,t) = \frac{1}{\sqrt{2}}(\psi_0(R,x,y)e^{-iE_0 t} + \psi_1(R,x,y)e^{-iE_1 t}) \tag{34}$$

with the respective eigenvalues E_0 and E_1. By solving the electronic problem at each nuclear configuration, we obtain the Born−Oppenheimer potentials $\epsilon_j^{BO}(R)$ and electronic states $\phi_j^{BO}(x,y|R)$. The lowest potential energy surfaces are shown in Figure 1 together with the initial wave function. The ground state is a double-well potential that is energetically separated from the excited states. Its lowest two vibrational states are used to construct the time-dependent Born−Oppenheimer nuclear wave function as

$$\chi^{BO}(R,t) = \frac{1}{\sqrt{2}}(\chi_{0,0}^{BO}(R)e^{-iE_{0,0}^{BO} t} + \chi_{0,1}^{BO}(R)e^{-iE_{0,1}^{BO} t}) \tag{35}$$

where $E_{0,0}^{BO}$ and $E_{0,1}^{BO}$ are the respective eigenenergies. Although for the mass ratios that we use there is a small difference between exact and Born−Oppenheimer eigenvalues, this difference only changes the tunneling time but does not influence the tunneling dynamics in any other way. Hence, it will not be noticeable below, because we will always consider the time in units of the tunneling time for both the exact and the Born−Oppenheimer dynamics.

First, we analyze the expansion parameter $\lambda(R,t)$, (21) and (23), shown in Figure 2. The real part of λ corresponds to the velocity field and shows the typical behavior that occurs in coherent tunneling in a symmetric double-well potential: The velocity is everywhere almost zero except under the barrier, where it can have large values.[55] The imaginary part of λ, which

DOI: 10.1021/acs.jpca.5b12657
J. Phys. Chem. A 2016, 120, 3316−3325

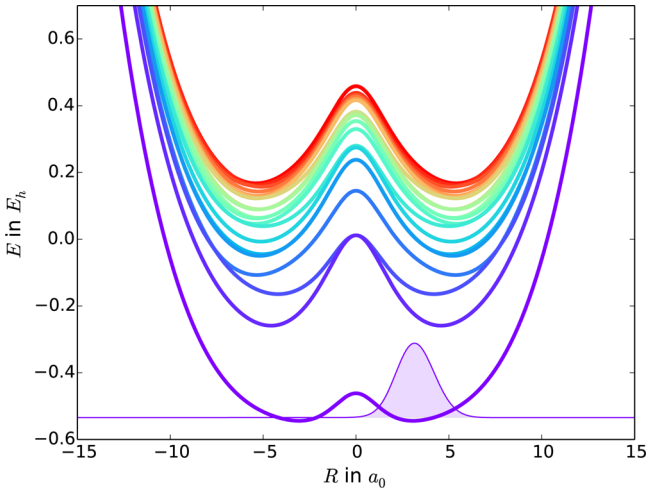

Figure 1. Lowest 20 Born−Oppenheimer potential energy surfaces and initial Born−Oppenheimer wave function for the tunneling dynamics (superposition of the lowest two eigenstates of the ground state potential), for a nucleus with mass 50 m_e. For the over-the-barrier dynamics, this state was shifted by 4.5 a_0 to the right.

is basically the gradient of the density divided by the density, has nonzero (albeit small) values both in the region of the barrier and away from the minimum. Thus, λ is close to zero in the relevant region around the minima, where the wave function is always localized during coherent tunneling.

After one-quarter of the tunneling time, the density is localized equally in both potential wells. Figure 3 shows the nuclear density and flux density, as well as the electron density and flux density, at that time. The dynamics started in the right potential well; hence, the nuclear flux density is negative, representing a motion to the left. The electron density is also equally distributed between the two wells. The electronic flux density has characteristics similar to those of the nuclear one: It is strongest in the region of the barrier, and it is directed to the left well.

In Figure 3, next to the exact electronic density and flux density, also the NVPT density and flux density are shown for λ^{BO} and assuming classical nuclei at the expectation value of position and momentum. We will now discuss how these compare to the exact quantities.

The NVPT correction $\Phi^{(1)}$ was obtained from (27) with the ground state BO surface and BO electronic wave function. Also, λ^{BO} is λ defined in (21) but evaluated by using the BO nuclear wave function χ^{BO} instead of the exact one, as λ^{BO} is the one that is available in practice.

From the figure, it is clear that exact and NVPT electronic density and flux density are in almost perfect agreement. To assess the quality of the NVPT flux density, we define an error measure

$$E_x(t) = \frac{1}{n_x} \sum_k \left| \frac{j_{x,k} - j_{x,k}^{\mathrm{NVPT}}}{j_{x,k}} \right| \qquad \text{for } |\mathbf{j}| > 0.1 \max|\mathbf{j}| \tag{36}$$

where $j_{x,k} = [\mathbf{j}(x_k)]_x$ is the x-component of the flux density, evaluated at grid point x_k. The error measure has the meaning of an average relative error. To exclude the large relative errors at small magnitudes $|\mathbf{j}|$ of the flux density, we restrict the set of points x_k to the points where $|\mathbf{j}(x_k)|$ is at least 10% of the maximum magnitude at the given time. We also only consider the x-direction, because the flux in the y-direction is very small for the considered dynamics. Additionally, to single out the error of NVPT as compared to the error of the dynamics introduced by the BO approximation, we compute the NVPT flux density with the parameter λ computed from the exact wave function.

Figure 4 shows the errors of the electronic flux density with respect to the number of excited states used in (28), and the error if the correction is obtained directly from (27). The error was computed for different masses of the heavy particle. The errors for coherent tunneling do not depend on time (except if the flux density becomes very small, for numerical reasons).

It can be seen that, except for mass $M = 10\ m_e$, the errors for different nuclear masses are very similar. There are steps in the

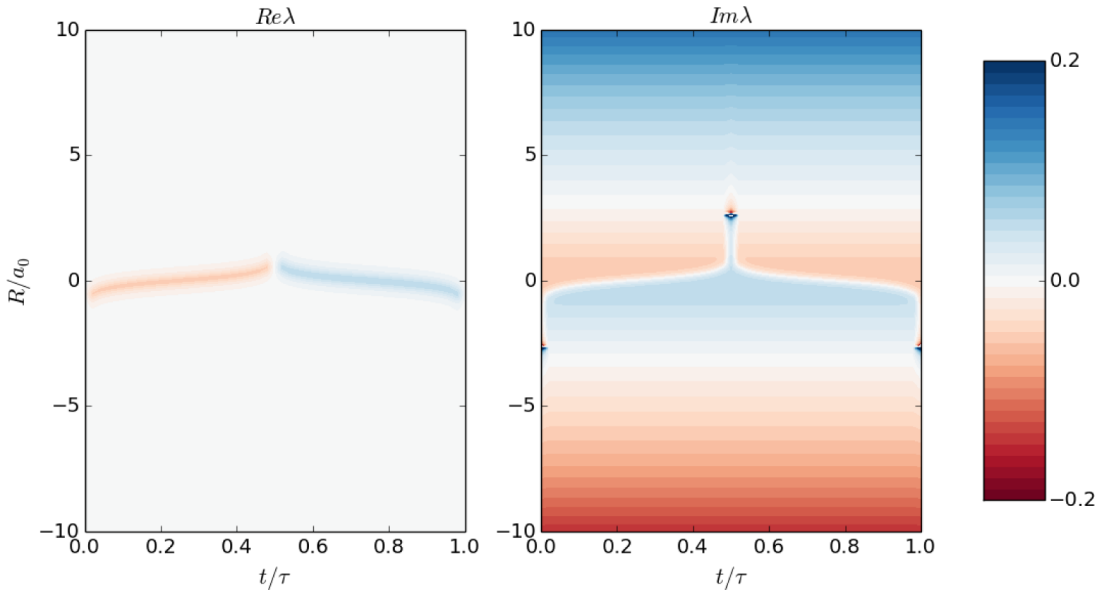

Figure 2. Real (left) and imaginary (right) part of the expansion parameter λ for the tunneling dynamics, for a nucleus with mass 50 m_e.

DOI: 10.1021/acs.jpca.5b12657
J. Phys. Chem. A 2016, 120, 3316−3325

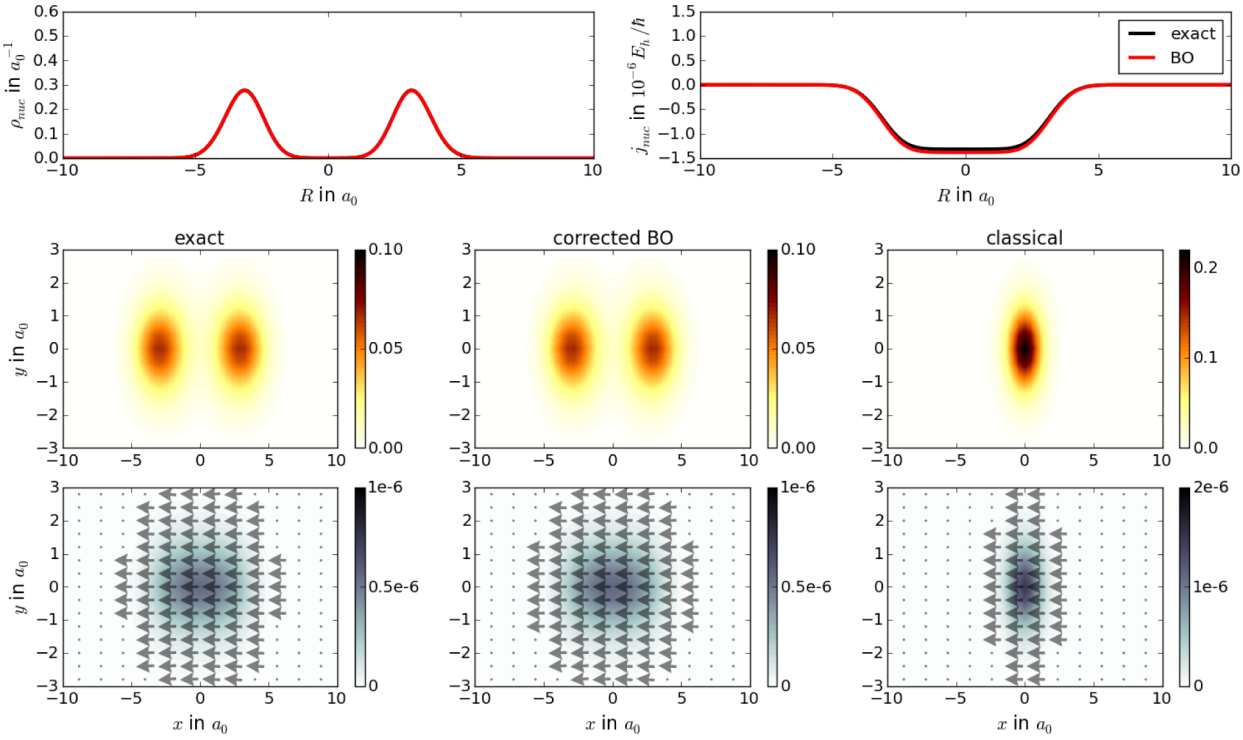

Figure 3. Top: nuclear density (left) and flux density (right) for the exact nuclear wave function χ and for the Born−Oppenheimer (BO) nuclear wave function χ^{BO}, after one-quarter of the tunneling time, for a nucleus with mass 50 m_e. Below: electron density (top) and flux density (below, with contours indicating the magnitude and arrows indicating the direction, for points where the flux is more than 1% of its maximum value) at that time for the exact wave function (left), for the BO electronic wave function corrected by nuclear velocity perturbation theory (NVPT, center), and for the NVPT electronic wave function at the expectation value of nuclear position and momentum (right).

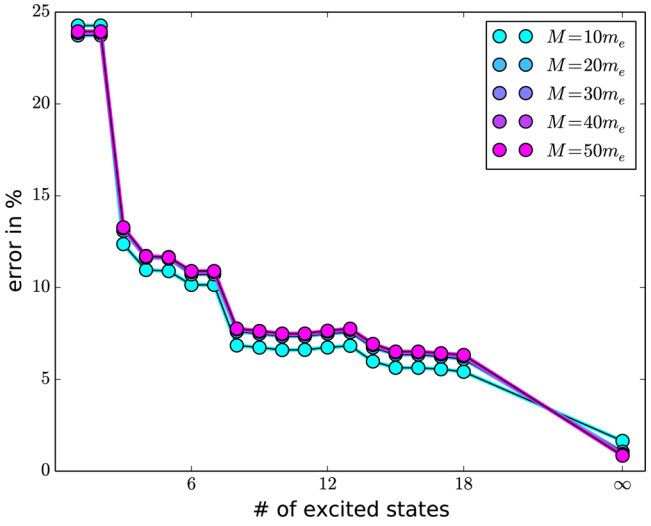

Figure 4. Average relative error of the x-component of the electronic flux density obtained from nuclear velocity perturbation theory during coherent tunneling for several masses of the nucleus. The number of states indicates how many states were taken into account for computing the correction according to (28), and ∞ means computation of the correction according to (27). The errors do not change with time.

convergence with respect to the number of excited states. The steps can be explained with the nonadiabatic coupling vectors d_{j0}. By the symmetry of our system, we can expect that every second of these coupling vectors is zero. However, there are avoided crossings in the excited states so that the character of the state changes along the nuclear coordinate, and hence some of the coupling vectors are zero for some regions along R. Specifically, the coupling to the first excited state d_{10} is nowhere zero; hence, inclusion of this contribution to the electronic wave function is significant. In contrast, d_{20} is zero in the region $|R| < 7.7\ a_0$. At $R = 7.7\ a_0$ there is an avoided crossing in the BO surfaces and for $|R| > 7.7\ a_0$ the coupling d_{20} is not zero, but it is also not relevant for the dynamics. Hence, there is almost no contribution of the second excited state to the flux density and the error does not decrease. For higher excited states the situation is similar but more complicated due to the presence of further avoided crossings. Otherwise, we find that already inclusion of only the first excited state yields a flux density that can be used for qualitative analysis. The flux density obtained from solving (27), which formally includes all excited states, shows that the error made by including only first-order terms in the expansion coefficient λ is negligible for any but the most accurate simulations.

Additionally, in ab-inito molecular dynamics simulations the nuclei are treated (semi-)classically and hence, instead of a nuclear wave function, only a nuclear position and velocity is available. To study the electronic flux density in this case, too, we define a classical wave function

$$\Psi^{cl}(x,y,t) = \Phi^{(0)}(x,y|\langle R\rangle(t)) + \frac{\langle -i\hbar\partial_R\rangle(t)}{M}\Phi^{(1)}(x,y|\langle R\rangle(t)) \quad (37)$$

where $\langle R\rangle(t)$ and $\langle -i\hbar\partial_R\rangle(t)$ are the time-dependent nuclear position and momentum expectation values, respectively. Figure 3 shows that the classical NVPT electronic flux density is too localized and has too large a magnitude as compared to

DOI: 10.1021/acs.jpca.5b12657
J. Phys. Chem. A 2016, 120, 3316−3325

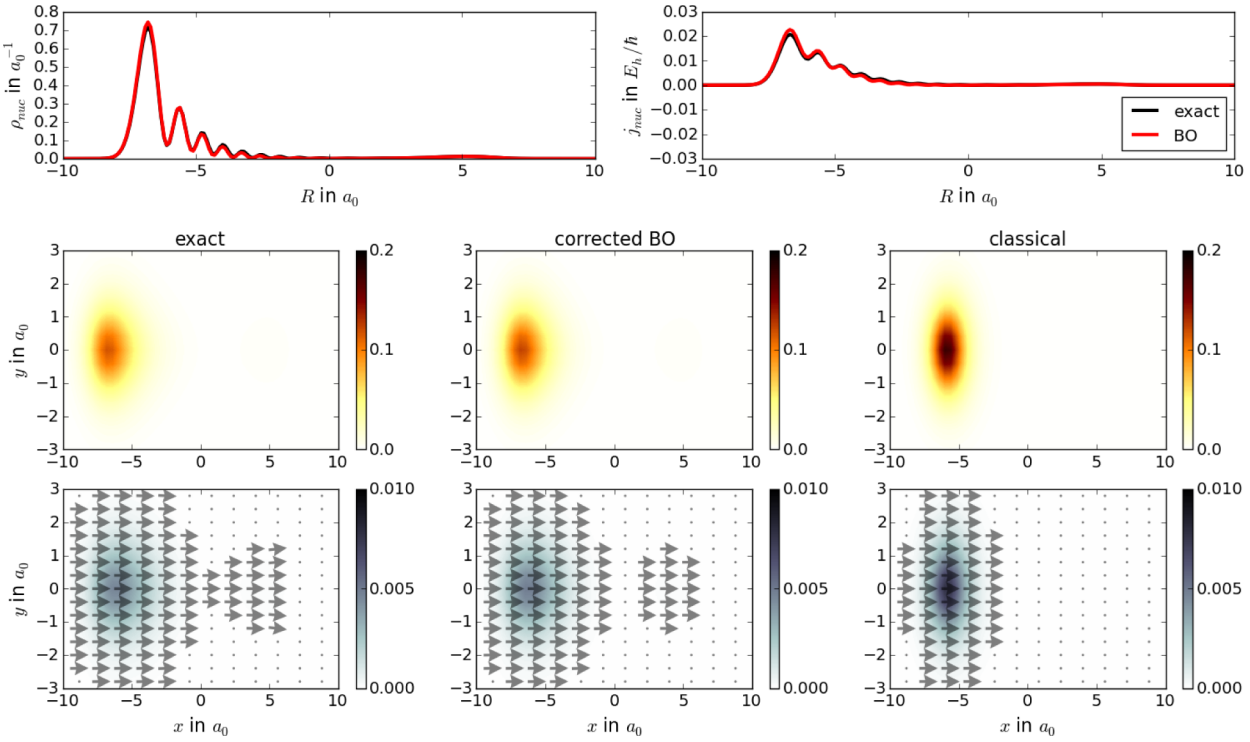

Figure 5. Like Figure 3, but for the over-the-barrier dynamics. The initial state corresponds to the nuclear wavepacket of Figure 1, shifted by 4.5 a_0 to the right. It moves to the left potential well, hits the potential wall, and is backscattered. The figure shows the quantities at a time shortly after the backscattering.

the exact one. As the preceding discussion shows, this is not the failure of the NVPT, but rather of replacing the density that is localized at the two potential wells by a density at the position expectation value.

Over-the-Barrier Dynamics. As a second example, we consider the scattering of a wavepacket at the barrier. Our initial state is the same wave function as for the tunneling case, i.e., a superposition of ground and first excited state of the full system. This time, however, we shift the state by 4.5 a_0 in the R-direction, so that it is initially localized around R = 7.7 a_0. A classical nucleus localized at this position has enough energy to overcome the barrier, as can be seen from Figure 1. The nuclear wavepacket dynamics shows initially a motion to the left. When the wavepacket hits the barrier, it is backscattered by a small amount but mostly continuing to the left, where it scatters an the left potential wall and is reflected.

We consider a nucleus of mass 50 m_e and a time t right after the dominant part of the wavepacket had hit the left potential wall and returns to the right. Figure 5 shows the densities and flux densities at that time.

From the nuclear density and flux density we see that the main part of the wavepacket is left of R = 0 and its motion is directed to the right. There is also a small part around R = 5 a_0 that is also directed to the right. This part has previously been backscattered at the barrier. The same behavior is found for the electrons, albeit from the figure of the exact electron density this is not apparent. However, for the exact electronic flux density we plotted the directional arrows for all points where the magnitude of the flux density is larger than 1% of the maximum magnitude. The arrows around x = 4 a_0 show the backscattering also in the electronic part.

The NVPT electronic density and flux density show almost quantitative agreement also for this dynamics. We again analyzed the errors, but not with respect to a change in mass but only during the time evolution.

Figure 6 shows the results. In contrast to the coherent tunneling dynamics, the errors of the over-the-barrier dynamics change with time. We see nevertheless a similar behavior of the error with respect to the number of included excited states like in the tunneling case. However, for inclusion of the lowest few excited states the error varies with time significantly: At certain

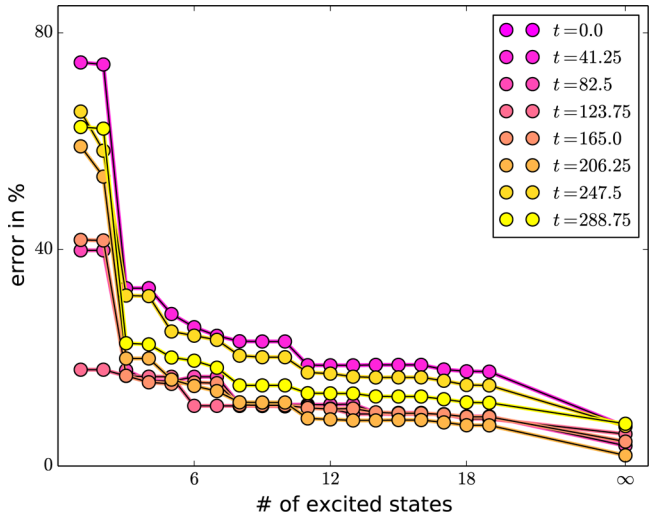

Figure 6. Like Figure 4, but for the over-the-barrier dynamics and only for a nucleus with mass 50 m_e. The error is shown at several different times during which the wavepacket moves from its initial position in the right potential well to the left well and is backscattered. The last time corresponds to the situation of Figure 5. All times are given in $\hbar/E_h$.

DOI: 10.1021/acs.jpca.5b12657
J. Phys. Chem. A 2016, 120, 3316−3325

times, inclusion of only the first excited state in the determination of the electronic flux density seems to be enough, with only little improvement from further states. However, for most time steps, at least the lowest three states need to be taken into account for a quantitatively correct flux density. The error of the limiting case of formally including all excited state also varies with time and can be up to 5%. Thus, also the quality of the flux density including only first-order terms of λ varies slightly.

Lastly, we find that the classical flux density shows the correct qualitative behavior, although too localized and with a slightly too high magnitude. The localization is a result of replacing the true electron density by the density corresponding to the position expectation value. Nevertheless, if the nuclear wavepacket is adequately represented by its expectation values, and if the BO approximation is valid, the NVPT electronic flux density can be expected to give a qualitatively correct picture.

CONCLUSIONS

In this article, we showed that the electronic flux density obtained from NVPT is adequate for BO dynamics. Seen from the exact factorization, it can be derived from a perturbation expansion in the same parameter that also has to be small for the BO approximation to hold. For a model system involving a nucleus and an electron in an external potential, we find that the NVPT electronic flux density yields quantitative results if the correction is determined by solving a system of equations that only involves the ground electronic potential and wave function. Alternatively, if information about electronically excited states is available, the information can also be used to obtain an estimate of the electronic flux density. This may be a valuable alternative when only the qualitative reaction mechanism of a chemical rearrangement is of interest. Whenever a classical description of nuclei represents the nuclear dynamics well, the NVPT flux density using only the classical velocity also represents the exact one well. Finally, it can be used to include nuclear quantum effects in the electronic flux density.

Computation of the NVPT electronic flux density from the ground state properties is computationally not prohibitive for molecules. However, although for the case of classical nuclei the correction was known in the theory of vibrational circular dichroism for some time,[23] it was implemented only recently for a plane-wave basis set[19] and has not yet been implemented in an atom-centered basis set because the implementation has many caveats.[6] As the electronic flux density is a very useful quantity and the NVPT correction is a good way to obtain it for the dynamics of molecules, we hope to stimulate further research for its practical implementation.

AUTHOR INFORMATION

Corresponding Author

*A. Schild. E-mail: aschild@mpi-halle.mpg.de.

Notes

The authors declare no competing financial interest.

ACKNOWLEDGMENTS

Partial support from the Deutsche Forschungsgemeinschaft (SFB 762) and from the European Commission (FP7-NMP-CRONOS) is gratefully acknowledged.

ADDITIONAL NOTE

[a]The Born−Oppenheimer approximation may also mean that several nuclear wave functions evolve on Born−Oppenheimer surfaces ϵ_j^{BO} independently. Here, we will only consider the ground state.

REFERENCES

(1) Born, M.; Oppenheimer, R. J. Zur Quantentheorie der Molekeln. *Ann. Phys.* **1927**, *389*, 457−484.
(2) Barth, I.; Hege, H.-C.; Ikeda, H.; Kenfack, A.; Koppitz, M.; Manz, J.; Marquardt, F.; Paramonov, G. K. Concerted quantum effects of electronic and nuclear fluxes in molecules. *Chem. Phys. Lett.* **2009**, *481*, 118−123.
(3) Bredtmann, T.; Diestler, D. J.; Li, S.-D.; Manz, J.; Pérez-Torres, J. F.; Tian, W.-J.; Wu, Y.-B.; Yang, Y.; Zhai, H.-J. Quantum theory of concerted electronic and nuclear fluxes associated with adiabatic intramolecular processes. *Phys. Chem. Chem. Phys.* **2015**, *17*, 29421−29464.
(4) Nagashima, K.; Takatsuka, K. Electron-Wavepacket Reaction Dynamics in Proton Transfer of Formamide. *J. Phys. Chem. A* **2009**, *113*, 15240−15249.
(5) Becke, A. D.; Edgecombe, K. E. A simple measure of electron localization in atomic and molecular systems. *J. Chem. Phys.* **1990**, *92*, 5397.
(6) Nafie, L. A. *Vibrational Optical Activity: Principles and Applications*; Wiley: New York, 2011.
(7) Okuyama, M.; Takatsuka, K. Electron flux in molecules induced by nuclear motion. *Chem. Phys. Lett.* **2009**, *476*, 109−115.
(8) Pohl, V.; Tremblay, J.-C. Adiabatic electronic flux density: a Born−Oppenheimer Broken Symmetry ansatz. *Phys. Rev. A* **2016**, *93*, 012504.
(9) Diestler, D. J. Coupled-Channels Quantum Theory of Electronic Flux Density in Electronically Adiabatic Processes: Fundamentals. *J. Phys. Chem. A* **2012**, *116*, 2728−2735.
(10) Diestler, D. J.; Kenfack, A.; Manz, J.; Paulus, B. Coupled-Channels Quantum Theory of Electronic Flux Density in Electronically Adiabatic Processes: Application to the Hydrogen Molecule Ion. *J. Phys. Chem. A* **2012**, *116*, 2736−2742.
(11) Diestler, D. J.; Kenfack, A.; Manz, J.; Paulus, B.; Pérez-Torres, J. F.; Pohl, V. Computation of the Electronic Flux Density in the Born-Oppenheimer Approximation. *J. Phys. Chem. A* **2013**, *117*, 8519−8527.
(12) Hermann, G.; Paulus, B.; Pérez-Torres, J. F.; Pohl, V. Electronic and nuclear flux densities in the H_2 molecule. *Phys. Rev. A: At., Mol., Opt. Phys.* **2014**, *89*, 052504.
(13) Diestler, D. J. Quasi-Classical Theory of Electronic Flux Density in Electronically Adiabatic Molecular Processes. *J. Phys. Chem. A* **2012**, *116*, 11161−11166.
(14) Diestler, D. J. Beyond the Born-Oppenheimer Approximation: A Treatment of Electronic Flux Density in Electronically Adiabatic Molecular Processes. *J. Phys. Chem. A* **2013**, *117*, 4698−4708.
(15) Bredtmann, T.; Manz, J. Electronic Bond-to-Bond Fluxes in Pericyclic Reactions: Synchronous or Asynchronous? *Angew. Chem., Int. Ed.* **2011**, *50*, 12652−12654.
(16) Bredtmann, T.; Manz, J. Elektronenflüsse zwischen benachbarten Bindungen bei pericyclischen Reaktionen: synchron oder asynchron? *Angew. Chem.* **2011**, *123*, 12863−12866.
(17) Schild, A.; Choudhary, D.; Sambre, V. D.; Paulus, B. Electron Density Dynamics in the Electronic Ground State: Motion Along the Kekul Mode of Benzene. *J. Phys. Chem. A* **2012**, *116*, 11355−11360.
(18) Manz, J.; Yamamoto, K. A selection rule for the directions of electronic fluxes during unimolecular pericyclic reactions in the electronic ground state. *Mol. Phys.* **2012**, *110*, 517−530.
(19) Scherrer, A.; Vuilleumier, R.; Sebastiani, D. Nuclear Velocity Perturbation Theory of Vibrational Circular Dichroism. *J. Chem. Theory Comput.* **2013**, *9*, 5305.
(20) Scherrer, A.; Agostini, F.; Sebastiani, D.; Gross, E. K. U.; Vuilleumier, R. Nuclear velocity perturbation theory for vibrational

DOI: 10.1021/acs.jpca.5b12657
J. Phys. Chem. A 2016, 120, 3316−3325

circular dichroism: An approach based on the exact factorization of the electron-nuclear wave function. *J. Chem. Phys.* **2015**, *143*, 074106.
(21) Abedi, A.; Maitra, N. T.; Gross, E. K. U. Exact Factorization of the Time-Dependent Electron-Nuclear Wave Function. *Phys. Rev. Lett.* **2010**, *105*, 123002.
(22) Abedi, A.; Maitra, N. T.; Gross, E. K. U. Correlated electron-nuclear dynamics: Exact factorization of the molecular wave-function. *J. Chem. Phys.* **2012**, *137*, 22A530.
(23) Nafie, L. A. Adiabatic molecular properties beyond the Born-Oppenheimer approximation. Complete adiabatic wave functions and vibrationally induced electronic current density. *J. Chem. Phys.* **1983**, *79*, 4950−4957.
(24) Patchkovskii, S. Electronic currents and Born-Oppenheimer molecular dynamics. *J. Chem. Phys.* **2012**, *137*, 084109.
(25) Scherrer, A.; Vuilleumier, R.; Sebastiani, D. Nuclear Velocity Perturbation Theory of Vibrational Circular Dichroism. *J. Chem. Theory Comput.* **2013**, *9*, 5305−5312.
(26) Littlejohn, R. G.; Reinsch, M. Gauge fields in the separation of rotations and internal motions in the *n*-body problem. *Rev. Mod. Phys.* **1997**, *69*, 213−276.
(27) Sutcliffe, B. Some difficulties in considering rotation motion within the Born-Oppenheimer approximation for polyatomic molecules. *Int. J. Quantum Chem.* **2012**, *112*, 2894−2903.
(28) Gidopoulos, N. I.; Gross, E. K. U. Electronic non-adiabatic states: towards a density functional theory beyond the Born-Oppenheimer approximation. *Philos. Trans. R. Soc., A* **2014**, *372*, 20130059.
(29) Alonso, J. L.; Clemente-Gallardo, J.; Echeniche-Robba, P.; Jover-Galtier, J. A. Comment on "Correlated electron-nuclear dynamics: Exact factorization of the molecular wave-function". *J. Chem. Phys.* **2013**, *139*, 087101.
(30) Abedi, A.; Maitra, N. T.; Gross, E. K. U. Reply to Comment on "Correlated electron-nuclear dynamics: Exact factorization of the molecular wave-function. *J. Chem. Phys.* **2013**, *139*, 087102.
(31) Abedi, A.; Agostini, F.; Suzuki, Y.; Gross, E. K. U. Dynamical Steps that Bridge Piecewise Adiabatic Shapes in the Exact Time-Dependent Potential Energy Surface. *Phys. Rev. Lett.* **2013**, *110*, 263001.
(32) Agostini, F.; Abedi, A.; Suzuki, Y.; Gross, E. K. U. Mixed quantum-classical dynamics on the exact time-dependent potential energy surfaces: A novel perspective on non-adiabatic processes. *Mol. Phys.* **2013**, *111*, 3625.
(33) Abedi, A.; Agostini, F.; Gross, E. K. U. Mixed quantum-classical dynamics from the exact decomposition of electron-nuclear motion. *Europhys. Lett.* **2014**, *106*, 33001.
(34) Agostini, F.; Abedi, A.; Gross, E. K. U. Classical nuclear motion coupled to electronic non-adiabatic transitions. *J. Chem. Phys.* **2014**, *141*, 214101.
(35) Agostini, F.; Abedi, A.; Suzuki, Y.; Min, S. K.; Maitra, N. T.; Gross, E. K. U. The exact electronic back-reaction on classical nuclei in non-adiabatic charge transfer. *J. Chem. Phys.* **2015**, *142*, 084303.
(36) Agostini, F.; Min, S. K.; Gross, E. K. U. Semiclassical analysis of the electron-nuclear coupling in electronic non-adiabatic processes. *Ann. Phys.* **2015**, *527*, 546.
(37) Min, S. K.; Abedi, A.; Kim, K. S.; Gross, E. K. U. Is the molecular Berry phase an artifact of the Born-Oppenheimer approximation? *Phys. Rev. Lett.* **2014**, *113*, 263004.
(38) Suzuki, Y.; Abedi, A.; Maitra, N. T.; Yamashita, K.; Gross, E. K. U. Electronic Schrödinger equation with nonclassical nuclei. *Phys. Rev. A: At., Mol., Opt. Phys.* **2014**, *89*, 040501(R).
(39) Suzuki, Y.; Abedi, A.; Maitra, N. T.; Gross, E. K. U. Laser-induced electron localization in H_2^+: Mixed quantum-classical dynamics based on the exact time-dependent potential energy surface. *Phys. Chem. Chem. Phys.* **2015**, *17*, 29271.
(40) Hunter, G. Conditional probability amplitudes in wave mechanics. *Int. J. Quantum Chem.* **1975**, *9*, 237−242.
(41) Czub, J.; Wolniewicz, L. On the non-adiabatic potentials in diatomic molecules. *Mol. Phys.* **1978**, *36*, 1301−1308.
(42) Hunter, G. Nodeless wave function quantum theory. *Int. J. Quantum Chem.* **1980**, *17*, 133−137.
(43) Hunter, G. Nodeless wave functions and spiky potentials. *Int. J. Quantum Chem.* **1981**, *19*, 755−761.
(44) Cederbaum, L. S. Born-Oppenheimer approximation and beyond for time-dependent electronic processes. *J. Chem. Phys.* **2008**, *128*, 124101.
(45) Chiang, Y.-C.; Klaiman, S.; Otto, F.; Cederbaum, L. S. The exact wavefunction factorization of a vibronic coupling system. *J. Chem. Phys.* **2014**, *140*, 054104.
(46) Min, S. K.; Agostini, F.; Gross, E. K. U. A coupled-trajectory quantum-classical approach to decoherence in non-adiabatic processes. *Phys. Rev. Lett.* **2015**, *115*, 073001.
(47) van Vleck, J. H. *Proc. Natl. Acad. Sci. U. S. A.* **1928**, *14*, 178.
(48) Requist, R.; Gross, E. K. U. Molecular geometric phase from the exact electron-nuclear factorization. arXiv:1506.09193 [physics.chem-ph], 2015.
(49) Hammes-Schiffer, S.; Stuchebrukhov, A. A. Theory of Coupled Electron and Proton Transfer Reactions. *Chem. Rev.* **2010**, *110*, 6939−6960.
(50) Pundt, A.; Kirchheim, R. HYDROGEN IN METALS: Microstructural Aspects. *Annu. Rev. Mater. Res.* **2006**, *36*, 555−608.
(51) *SciPy sparse linear algebra package*, http://docs.scipy.org/doc/scipy-dev/reference/sparse.linalg.html.
(52) Lehoucq, R. B.; Sorensen, D. C.; Yang, C. *ARPACK USERS GUIDE: Solution of Large Scale Eigenvalue Problems by Implicitly Restarted Arnoldi Methods*; SIAM: Philadelphia, PA, 1998.
(53) Al-Mohy, A. H.; Higham, N. J. Computing the Action of the Matrix Exponential, with an Application to Exponential Integrators. *SIAM J. Sci. Comput.* **2011**, *33*, 488−511.
(54) Higham, N. J.; Al-Mohy, A. H. Computing Matrix Functions. *Acta Numer.* **2010**, *19*, 159−208.
(55) Manz, J.; Schild, A.; Schmidt, B.; Yang, Y. Maximum tunneling velocities in symmetric double well potentials. *Chem. Phys.* **2014**, *442*, 9−17.

DOI: 10.1021/acs.jpca.5b12657
J. Phys. Chem. A 2016, 120, 3316−3325